JACS
JOURNAL OF THE AMERICAN CHEMICAL SOCIETY

Article

pubs.acs.org/JACS

Functionalization of Boron Diiminates with Unique Optical Properties: Multicolor Tuning of Crystallization-Induced Emission and Introduction into the Main Chain of Conjugated Polymers

Ryousuke Yoshii, Amane Hirose, Kazuo Tanaka,* and Yoshiki Chujo*

Department of Polymer Chemistry, Graduate School of Engineering, Kyoto University, Katsura, Nishikyo-ku, Kyoto 615-8510, Japan

Supporting Information

ABSTRACT: In this article, we report the unique optical characteristics of boron diiminates in the solid states. We synthesized the boron diiminates exhibiting aggregation-induced emission (AIE). From the series of optical measurements, it was revealed that the optical properties in the solid state should be originated from the suppression of the molecular motions of the boron diiminate units. The emission colors were modulated by the substitution effects ($\lambda_{PL,crystal}$ = 448−602 nm, $\lambda_{PL,amorphous}$ = 478−645 nm). Strong phosphorescence was observed from some boron diiminates deriving from the effects of two imine groups. Notably, we found some of boron diiminates showed crystallization-induced emission (CIE) properties derived from the packing differences from crystalline to amorphous states. The 15-fold emission enhancement was observed by the crystallization ($\Phi_{PL,crystal}$ = 0.59, $\Phi_{PL,amorphous}$ = 0.04). Next, we conjugated boron diiminates with fluorene. The synthesized polymers showed good solubility in the common solvents, film formability, and thermal stability. In addition, because of the expansion of main-chain conjugation, the peak shifts to longer wavelength regions were observed in the absorption/emission spectra of the polymers comparing to those of the corresponding boron diiminate monomers (λ_{abs} = 374−407 nm, λ_{PL} = 509−628 nm). Furthermore, the absorption and the emission intensities were enhanced via the light-harvesting effect by the conjugation with fluorene. Finally, we also demonstrated the dynamic reversible alterations of the optical properties of the polymer thin films by exposing to acidic or basic vapors.

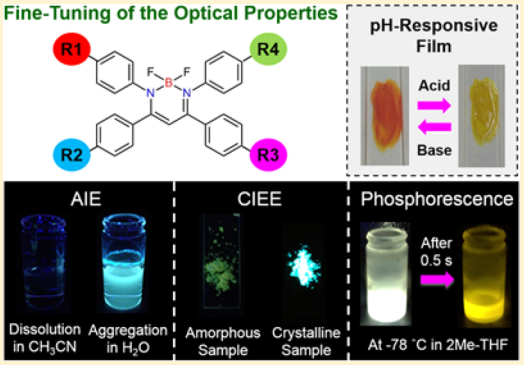

INTRODUCTION

Organoboron dyes and polymers are a versatile platform for fabricating opto and/or electric devices because of their superior properties such as light absorption, emission, high stability, and the electron acceptability.[1] For example, Jäkle et al. and Yamaguchi et al. have presented that organoboron dyes and organoboron-containing polymers show the multiple functions such as low-lying LUMOs, strong emissions, and high-electron-transport properties, respectively.[2,3] Fraser et al. have reported the versatile properties of boron diketonates involving prominent fluorescence, room temperature phosphorescence, and reversible mechanochromic fluorescence between the solid and the melt states.[4] So far, various smart optical materials have been developed based on organoboron complexes. Although most of the boron complexes exhibited strong emissions in the solution states, their emissions in the solid states were usually spoiled by intermolecular $\pi-\pi$ stacking interaction, called as aggregation-caused quenching (ACQ) effects.[5] The applications of organoboron dyes such as for advanced light-emitting devices or sensor materials are still limited by the ACQ effects.

Aggregation-induced emission (AIE) is a key phenomenon for overcoming the ACQ effect and obtaining highly efficient light-emitting solid materials. Tang et al. have reported a series of π-conjugated molecules that were nonemissive in the solution states but significantly emissive in the aggregate states.[6] Boron ketoiminates were also found as AIE-active molecules.[7] In particular, we have recently presented that ACQ-active organoboron dyes composed of the β-diketonate structure can be transformed to the AIE-active dyes by replacing one of the oxygen atoms in the β-diketonate ligand to nitrogen to form the ketoiminate structure.[7a] In the solid state, the molecular motions at the boron-chelating ring, which induced the emission quenching, should be suppressed. Thereby, significant emission was observed only from the aggregate state of the boron ketoiminate dyes. We also reported that the AIE behavior of boron ketoiminates can maintain in the main chain of the polymer. As a result, we obtained the AIE-active polymers composed of the boron ketoiminate units.[8] Furthermore, their photoluminescence (PL) can be tuned by modulating the substituents on the nitrogen atom.[9] These observations suggest that the boron ketoiminate derivatives should be a prominent solid-state emissive material and a useful building block for constructing highly emissive conjugated polymers.

Toward the next generations of AIE-active dyes and polymers with further functionality, we focused on the

Received: October 25, 2014
Published: December 18, 2014

dx.doi.org/10.1021/ja510985v | J. Am. Chem. Soc. 2014, 136, 18131−18139

Chart 1. Boron Diiminate Derivatives

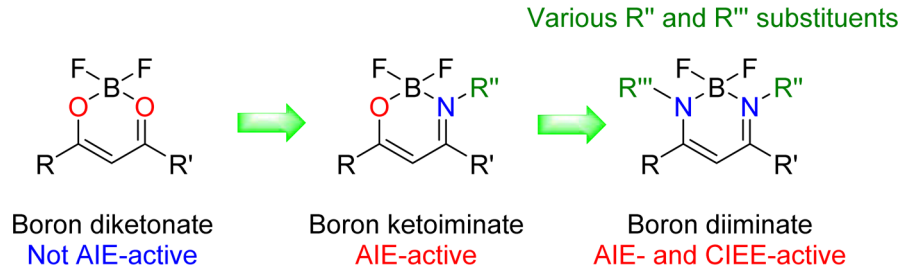

Scheme 1. Synthetic Routes for Compounds (a) 1 and (b) 3 and (c) the Boron Diiminates Derivatives

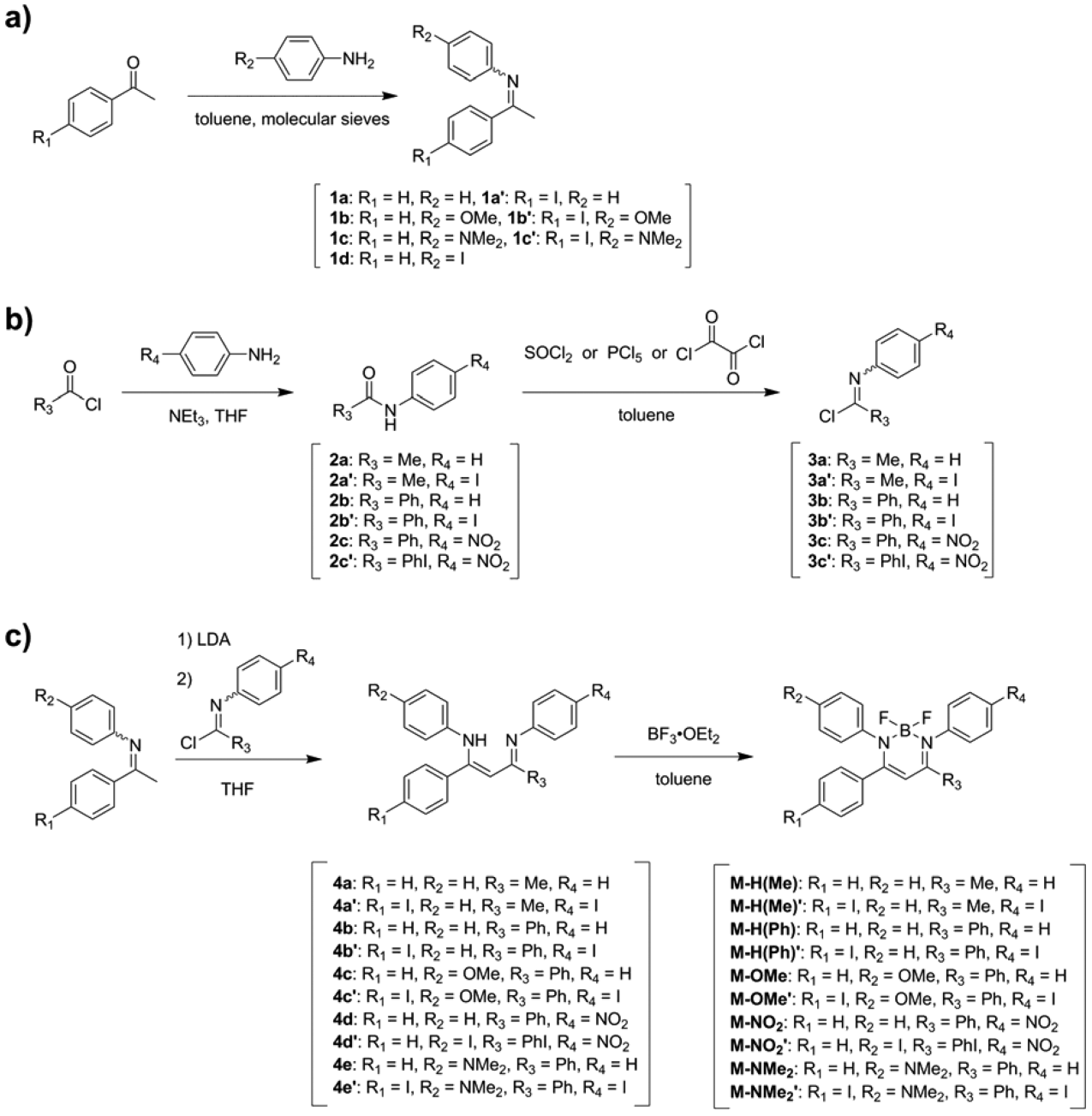

diiminate structure (Chart 1). Another functional group is acceptable at the nitrogen atom. Therefore, it can be expected that multiple functions are expressed due to the combination of those substituents as well as each intrinsic property. Indeed, we observed that the simple compounds of boron diiminates showed AIE behaviors similarly to the previous complexes.[10] In addition, the crystallization-induced emission enhancement (CIEE) property originated from the difference of the packing

dx.doi.org/10.1021/ja510985v | J. Am. Chem. Soc. 2014, 136, 18131−18139

Scheme 2. Synthetic Routes for the Boron Diiminate-Containing Polymers

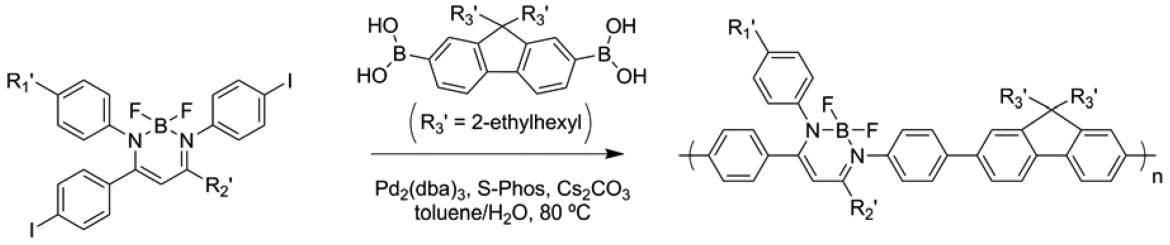

M-H(Me)': R_1' = H, R_2' = Me
M-H(Ph)': R_1' = H, R_2' = Ph
M-OMe': R_1' = OMe, R_2' = Ph
M-NO$_2$': R_1' =NO$_2$, R_2' = Ph
M-NMe$_2$': R_1' = NMe$_2$, R_2' = Ph

P-H(Me): R_1' = H, R_2' = Me
P-H(Ph): R_1' = H, R_2' = Ph
P-OMe: R_1' = OMe, R_2' = Ph
P-NO$_2$: R_1' =NO$_2$, R_2' = Ph
P-NMe$_2$: R_1' = NMe$_2$, R_2' = Ph

structure in the solid states was eventually obtained.[10] Thus, boron diiminates are potential units for receiving unique optical properties. However, the synthesis and the evaluation of the electronic structures of boron diiminate derivatives have been studied only in a few reports.[11] Especially, the effects on the conjugation with other functional units on the boron diiminates have been still unclear yet. The detailed study and the incorporation into the conjugation system should be required to clarify the intrinsic properties of boron diiminates and to apply for the optical materials.

Herein, we report the unique optical properties of the solid materials based on the boron diiminate-containing conjugated polymers. Initially, we prepared a series of boron diiminates and studied systematically the relationship between the substituents and their electronic structures. From the results of the optical measurements, it was found that all of the synthesized boron diiminates are AIE- and CIEE-active, and the emission colors of the crystallization-induced emission (CIE) can be drastically modulated from blue to orange by the alteration of the substituents. The significant enhancement (approximately 15-times) of the emission quantum yield was obtained by the crystallization. Next, based on these data, we synthesized the copolymers with the fluorene unit as a comonomer to offer the further functionalities of optical characteristics of boron diiminates through the main-chain conjugation.[12] Accordingly, boron diiminates-containing polymers showed strong absorption, higher emission efficiency, and red-shifted absorption/emission bands compared to the corresponding boron diiminates owing to the conjugation with fluorene. Moreover, the synthesized polymers possess material properties such as good solubility in common solvents, film-formability to form homogeneous films, and thermal stability. Finally, we also demonstrate the dynamic regulations of the optical properties of the polymer film based on the modulation of the electronegativity of the substituents using the acid−base treatments.

RESULTS AND DISCUSSION

Synthesis and Characterization. The diimine ligands **4a−e** with various substituents were synthesized via the reaction of *N*-phenylimine **1** and imidoyl chloride **3** with the corresponding substituents. The desired boron diiminates were prepared from the compounds **4a−e** by the boron-complexation using BF_3·OEt_2 (Scheme 1). Next, we prepared the copolymers with fluorene. The polymerization was accomplished by the palladium-catalyzed Suzuki−Miyaura coupling with [9,9-bis(2-ethylhexyl)-9H-fluorene-2,7-diyl]bisboronic acid and diiodo-substituted boron diiminates which were prepared according to the same reactions as other boron diiminates in the toluene water solvent mixture in the presence of 2-dicyclohexylphosphino-2′,6′-dimethoxybiphenyl (S-Phos) and tris(dibenzylideneacetone) dipalladium ($Pd_2(dba)_3$, Scheme 2). To improve the solubility of the products in common organic solvents, their numbers of repeating unit were limited to 20 by controlling the feed ratio of monomers. The terminal units of the synthesized polymers were capped with *p*-xylene units. While the synthesized polymers showed good solubility in nonpolar solvents such as THF, *o*-xylene, toluene, chloroform, and dichloromethane, they hardly dissolved in polar solvents such as MeOH, EtOH, AcOH, and acetonitrile. In addition, the homogeneous amorphous films were successfully prepared from the synthesized polymers by casting (Figure S4). The size exclusion chromatography (SEC) in $CHCl_3$ with the polystyrene standards revealed the number-average molecular weight (M_n) and the molecular weight distribution (M_w/M_n) of 26,000 and 3.3 for **P-H(Me)**, 13,200 and 2.9 for **P-H(Ph)**, 17,000 and 3.1 for **P-OMe**, 19,400 and 3.6 for **P-NO$_2$**, and 17,900 and 3.2 for **P-NMe$_2$**, respectively (Table 1). The chemical structures of the polymers were confirmed by ^{1}H, ^{13}C and ^{11}B NMR spectroscopies. All the purified compounds gave satisfactory spectroscopic data corresponding to their expected molecular structures (Figure S1−S3). The thermal properties of the synthesized compounds were investigated by thermogravimetric analysis (TGA) and differential scanning calorimetry (DSC). While the 5 wt % weight loss temperatures (T_{5d}) of boron diiminates attributable to the vaporization or the decomposition were observed at 266−298 °C, the polymers showed higher thermal stabilities (T_{5d} = 365−414 °C, Figure S5). In DSC measurements, the

Table 1. Physical Properties of Boron Fluorene Polymers[a]

compound	M_n	M_w	M_w/M_n	n[b]	yield (%)[c]
P-H(Me)	26,000	85,800	3.3	35	86
P-H(Ph)	13,200	38,300	2.9	16	83
P-OMe	17,000	52,700	3.1	20	92
P-NO$_2$	19,400	69,800	3.6	23	92
P-NMe$_2$	17,900	57.300	3.2	21	97

[a]Estimated by SEC with the polystyrene standards in $CHCl_3$. [b]Average number of repeating units calculated from M_n and molecular weights of repeating units. [c]Isolated yields after reprecipitation.

dx.doi.org/10.1021/ja510985v | J. Am. Chem. Soc. 2014, 136, 18131−18139

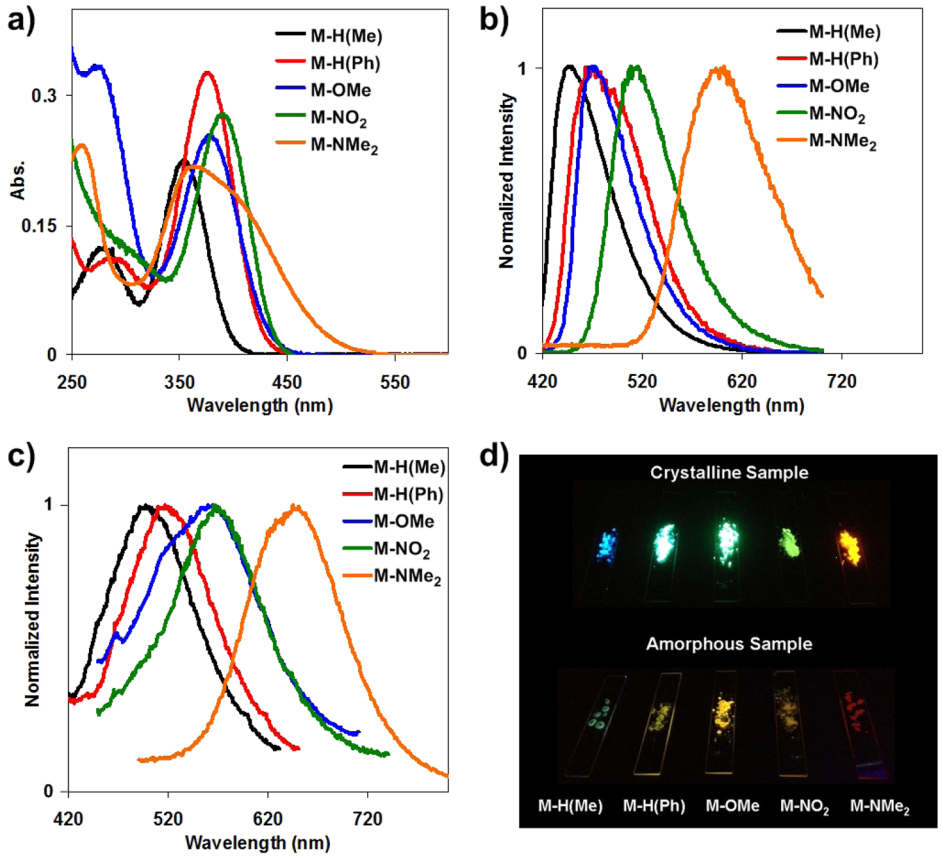

Figure 1. UV−vis absorption spectra of boron diiminates in (a) THF (1.0×10^{-5} M). PL spectra of the synthesized boron diiminates in (b) the crystalline states and in (c) the amorphous states upon the excitation at each absorption maximum. (d) Photographs of boron diiminates in crystalline and amorphous states under UV irradiation.

boron diiminates showed strong endothermic peaks as melting points around 173−261 °C. In contrast, the synthesized polymers hardly exhibited significant thermal transition peaks in the measurement temperature range from 0 to 300 °C (Figure S6 and Table S1). These observations strongly suggest that the copolymerization with the fluorene unit is an effective approach to improve the thermal stability and film formability of boron diiminates.

Optical and Electrochemical Properties of Boron Diiminates. The optical properties of the synthesized boron diiminates were investigated by a UV−vis absorption and PL spectroscopies (Figure 1). In UV−vis absorption spectra of the boron diiminates in THF (1×10^{-5} M, Figure 1a, Tables 2 and 3), they showed the strong absorption attributable to $\pi \rightarrow \pi^*$ transition at λ_{abs} = 355−391 nm. The values of the optical band gaps (E_g) which were estimated from the onset wavelength of the UV−vis spectra were in the order of **M-H(Me)** > **M-H(Ph)** > **M-OMe** > **M-NO$_2$** > **M-NMe$_2$**. **M-NMe$_2$** showed broader and red-shifted absorption than those of the others. It is implied that donor−acceptor interaction could be formed between the electron-donating amino unit and the electron-accepting boron chelating ring in **M-NMe$_2$**.

The electrochemical properties of the synthesized boron diiminates are summarized in Table 2. Their cyclic voltammograms (CV) are shown in Figure S7. Boron diiminates showed two or three reduction peaks. Their LUMO energy levels were estimated from the onsets of the first reduction waves by the empirical formula.[13] Their HOMO energy levels were calculated from LUMO energy levels and E_g of the corresponding compounds. All compounds showed low-lying LUMO energy levels in the region from −2.63 to −3.19 eV. It is suggested that boron diiminates work as an electron acceptor in the conjugation system. The chelation with a boron atom should induce the lowering effect.[8] Especially, **M-NO$_2$** exhibited the lowest-lying LUMO level than those of the other boron diiminates. This result can be explained by the effect of the nitro unit with the strong electron-accepting ability.

To theoretically support the optical and electrochemical behaviors of boron diiminates, density functional theory (DFT) calculations were carried out (Figure 2). The order of the HOMO−LUMO band gaps (E_g) and each energy level

Table 2. UV−vis Absorption and Electrochemical Properties of Boron Diiminates

compound	λ_{abs} [nm][a]	E_g [eV][b]	E_{red} [V][c,d]	HOMO [eV][e]	LUMO [eV][f]
M-H(Me)	355	3.12	−2.18	−5.75	−2.63
M-H(Ph)	376	2.91	−1.95	−5.77	−2.86
M-OMe	377	2.87	−1.98	−5.70	−2.83
M-NO$_2$	391	2.83	−1.62	−6.02	−3.19
M-NMe$_2$	365	2.54	−2.02	−5.33	−2.79

[a]UV−vis spectra were measured in THF (1.0×10^{-5} M). [b]The optical band gap estimated from the onset wavelength of the UV−vis spectra in THF. [c]CV was carried out in THF with 0.1 M Bu_4NPF_6 as supporting electrolyte. [d]E_{red} is the onset potential of first reduction wave (Figures S7 and S8). [e]Calculated from LUMO and optical band gap (E_g), HOMO = LUMO − E_g (eV). [f]Calculated from the empirical formula, LUMO = $-E_{red}$ − 4.80 (eV).[13]

dx.doi.org/10.1021/ja510985v | J. Am. Chem. Soc. 2014, 136, 18131−18139

Table 3. Optical Properties of Boron Diiminates[a]

compound	λ_{abs} [nm][b]	$\varepsilon \times 10^4$ [M^{-1} cm^{-1}][c]	$\lambda_{PL,cr}$ [nm][d]	$\lambda_{PL,am}$ [nm][e]	$\Phi_{PL,cr}$[d,f]	$\Phi_{PL,am}$[e,f]
M-H(Me)	355	2.26	448	478	0.11	0.02
M-H(Ph)	376	3.27	473	547	0.23	0.02
M-OMe	377	2.55	470	564	0.59	0.04
M-NO_2	391	2.79	509	568	0.04	0.01
M-NMe_2	365	2.19	602	645	0.08	0.01

[a]Excited at λ_{abs}. [b]Measured in THF (1×10^{-5} M). [c]Molar absorption coefficients of the absorption maxima at longer wavelength region. [d]Measured in crystalline states. [e]Measured in amorphous states. [f]Determined using integrated sphere method.

estimated from the DFT calculations showed similar trends to the experimental data estimated from the UV−vis absorption spectra and CV measurements. Furthermore, the existence of the intramolecular donor−acceptor interaction in **M-NMe_2** was proposed by the results from DFT calculations and CV measurements. These data mean that the substitution of an electron-donating amino unit led to the increase in the HOMO and the localization of the HOMO on the amino-substituted benzene. The LUMOs of the other boron diiminates (**M-H(Me)**, **M-H(Ph)**, **M-NO_2**) were delocalized through whole units. Meanwhile, the HOMOs were localized on a boron chelating ring and two phenyl units binding to nitrogen atoms. Thus, it is suggested that the energy levels of HOMO and LUMO should be strongly affected by the substituent on two phenyl units binding to the nitrogen atoms. On the other hand, the substituent binding to carbon atoms on the imine units should more effectively influence the LUMO than HOMO. In fact, although the HOMO of **M-H(Ph)** was hardly changed by the substitution of the phenyl unit in comparison with **M-H(Me)**, the LUMO was largely reduced by the substitution of benzene (Table 2 and Figure 2). These data indicate the HOMO and LUMO energy levels of boron diiminates can be efficiently modulated by the type of the substituents and the substitution positions.

The PL spectra of synthesized boron diiminates (1×10^{-5} M, Table 3) showed slight luminescence in THF ($\Phi < 0.01$). In contrast, crystallization led to large increases in their emission intensities. These results clearly indicate that the synthesized boron diiminates are AIE-active molecules. Next, the dependencies of the optical properties of the boron diiminates on temperature were examined (Figures S9−S13). In 2-methyltetrahydrofuran (2Me-THF), the emission intensities were much higher at low temperature (77 K) than those at room temperature (298 K). Since molecular motions such as torsion and vibration should be greatly suppressed under low temperature environments,[6c] the emission enhancement was observed at the low temperature. Furthermore, some boron diiminates showed dual emission bands attributable to fluorescence and phosphorescence at low temperature (Figures S9−13). According to the El-Sayed rule, when a change in spin multiplicity is accompanied by a change in electron configuration, the spin−orbit coupling is very large, and intersystem crossing is very rapid.[15] In addition, Fraser et al. have reported that boron diketonate derivatives including two

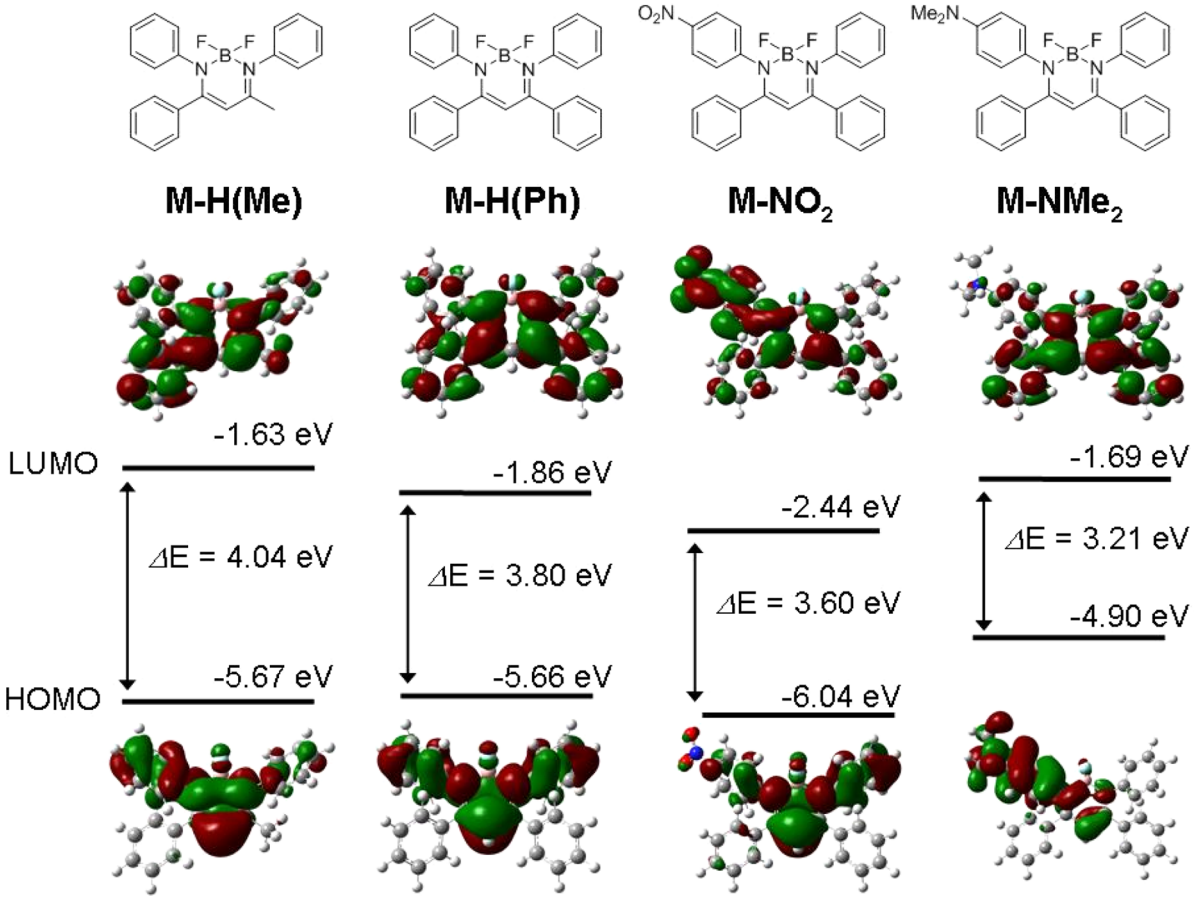

Figure 2. Structures and molecular orbital diagrams for the LUMO and HOMO of boron diiminates ((B3LYP/6-31G (d)//B3LYP/6-31G (d)).[14]

dx.doi.org/10.1021/ja510985v | J. Am. Chem. Soc. 2014, 136, 18131−18139

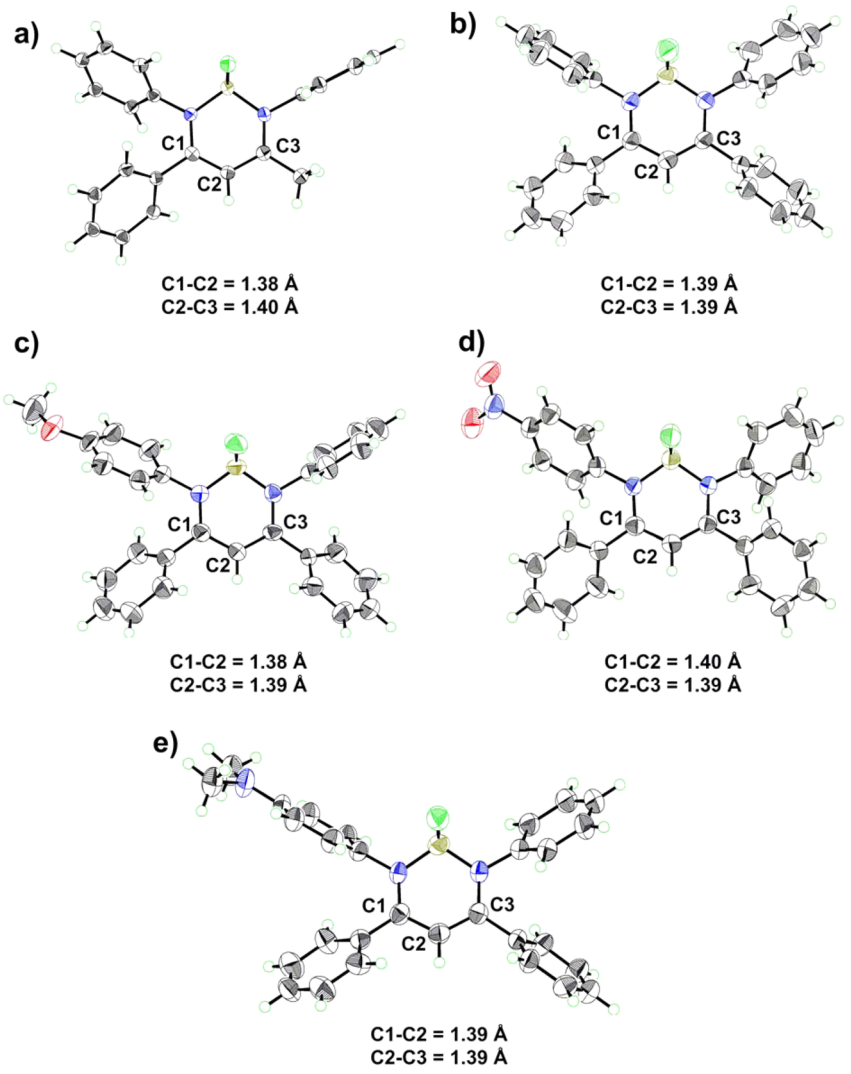

Figure 3. Molecular structures of (a) **M-H(Me)**, (b) **M-H(Ph)**, (c) **M-OMe**, (d) **M-NO_2**, and (e) **M-NMe_2**. Thermal ellipsoids are scaled to the 50% probability level.

carbonyl groups showed phosphorescence.[4a−c] Therefore, in this case, the existence of the lone-pair electrons on the two imine groups could be responsible for the strong phosphorescence. These observations suggest applicability of boron diiminates as phosphorescent materials and triplet sensitizers.

Next, the relationship between their morphologies and the emission properties in the solid state was investigated. Two types of solid samples were prepared. The crystal of boron diiminate was grown from MeOH. The amorphous sample was prepared by rapidly cooling the melted compound in a refrigerator at −20 °C.[6e,f] To examine the orientation of both samples in the solid state, we performed the powder X-ray diffraction (XRD). The XRD results of the crystal samples exhibited sharp and intense reflection patterns (Figure S4). These data indicate that the crystal samples involve ordered structures. In contrast, less clear reflections were observed in the amorphous samples. It was confirmed that the rapidly cooled samples should form amorphous states. In the PL spectra, the peak positions of the PL maxima (λ_{PL}) showed good correlation with the order of their E_g values. Strong emission was observed from the crystalline samples. On the other hand, the amorphous samples showed weaker emission in longer wavelength regions than those from the corresponding crystalline samples (Figure 1b,c and Table 3). Notably, the crystallization of **M-OMe** induced approximately 15-fold larger emission efficiencies from the amorphous state ($\Phi_{PL,crystal}$ = 0.59, $\Phi_{PL,amorphous}$ = 0.04). It is assumed that the formation of excimers via $\pi-\pi$ stacking of phenyl units, which often causes red-shifts of PL spectra and quenching, could be absent at the crystalline state.[6e,f] From these results, it is clearly shown that the synthesized boron diiminates are CIEE-active. Moreover, the colors of the CIE can be tuned from blue to red by the substituents.

X−Ray Crystal Structures of Boron Diiminates. The molecular conformations in the single crystals were investigated by X-ray analysis (Figures 3 and S14−S18 and Tables S2−S6). It was revealed that the lengths of C1−C2 and C2−C3 bonds in boron diiminates were hardly changed by the substituents. This fact suggests that the π-electrons on the boron-chelating ring could be delocalized in the diimine units regardless of the substituents. In the packing structures of boron diiminates, small degrees of $\pi-\pi$ interactions were observed between their phenyl rings. Since the boron diiminates showed shorter intermolecular CH···F distances (2.31−2.65 Å) than that of the sum of van der Waals radii (2.67 Å), the molecular conformation in the crystal could be stabilized and locked by

dx.doi.org/10.1021/ja510985v | J. Am. Chem. Soc. 2014, 136, 18131−18139

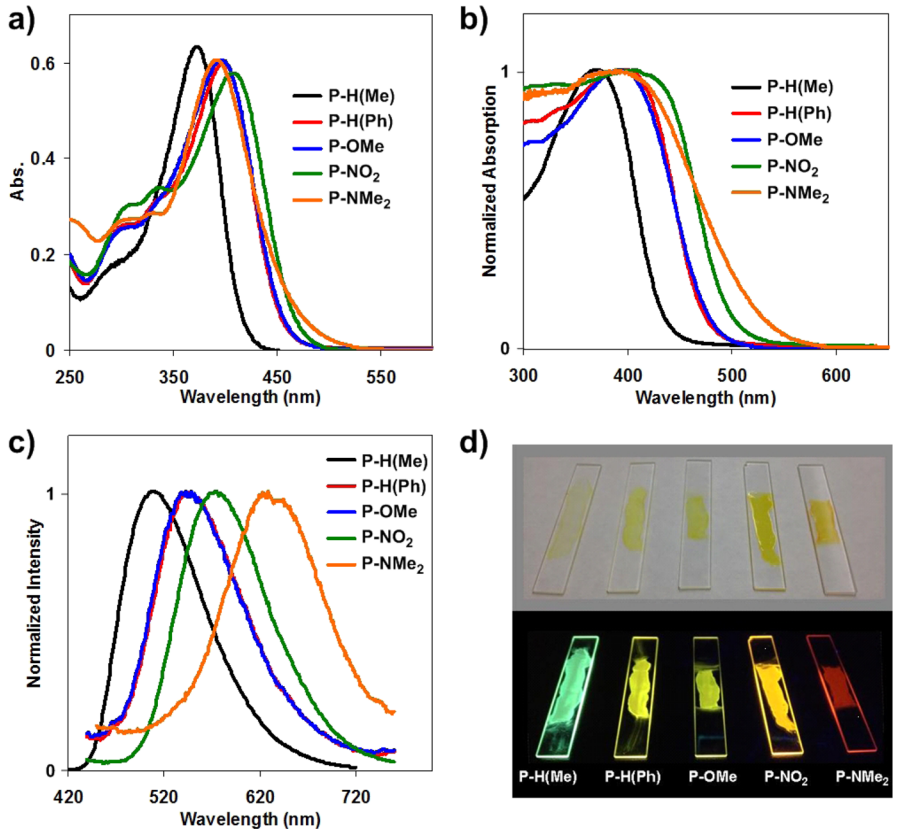

Figure 4. UV−vis absorption spectra of the synthesized polymers in (a) THF (1.0×10^{-5} M) and (b) the thin-film state. (c) PL spectra of the synthesized polymers in the thin-film state upon excitation at each absorption maximum. (d) Photographs of the synthesized polymers in the film state under the UV irradiation.

the multiple CH···F hydrogen bonds (Figures S14−S18). It is proposed that these interactions observed in the crystals could induce the blue-shifted emissions and the larger quantum yields of the crystal samples comparing to the amorphous samples.

Optical Properties of Boron Diiminate-Containing Polymers. The UV−vis absorption spectra of the synthesized polymers were recorded in THF (1×10^{-5} M, Figure 4a) and in thin-film states (Figure 4b). In the solution states, they showed red-shifted and stronger absorption bands assigned as $\pi-\pi^*$ transitions comparing to the corresponding boron diiminates (**M-H(Me)**, **M-H(Ph)**, **M-OMe**, **M-NO$_2$**, **M-NMe$_2$**). These results indicate that the π-conjugated systems were effectively elongated through the polymer main chains. In the case of thin-film sates, the polymers showed broader absorption than those in THF. It is suggested that interstrand interaction should be enhanced in the thin-film states.

The electrochemical properties of the polymers are summarized in Table 4. Their CVs are shown in Figure S8. The polymers showed clear reduction peaks, and most of the polymers exhibited lower-lying LUMO energy levels comparing to the corresponding boron diiminates. These data mean that the expansion of main-chain conjugation strongly influences the LUMO levels as the DFT calculations proposed (Figure 2). Moreover, it is proposed that the boron diiminate could work as an electron-accepting unit in the polymer since the fluorene unit has little electron acceptability. HOMO and LUMO of **P-NMe$_2$** exhibited almost same value as those of **M-NMe$_2$**. This fact indicates that the HOMO and LUMO in **P-NMe$_2$** have large contributions from the donor−acceptor system between the amino unit and the boron chelating ring than from the main-chain conjugation.

Table 4. UV−vis Absorption and Electrochemical Properties of the Polymers

compound	λ_{abs} [nm][a]	E_g [eV][b]	E_{red} [V][c,d]	HOMO [eV][e]	LUMO [eV][f]
P-H(Me)	374	2.99	−1.41	−6.34	−3.40
P-H(Ph)	399	2.73	−1.48	−6.06	−3.33
P-OMe	396	2.71	−1.94	−5.58	−2.87
P-NO$_2$	407	2.64	−1.51	−5.94	−3.30
P-NMe$_2$	392	2.53	−1.97	−5.37	−2.84

[a]UV−vis spectra of **CM**, **NM**, **CP**, and **NP** were measured in THF (1.0×10^{-5} M). [b]The optical band gap estimated from the onset wavelength of the UV−vis spectra in THF. [c]CV was carried out in THF with 0.1 M Bu_4NPF_6 as supporting electrolyte. [d]E_{red} is the onset potential of first reduction wave. [e]Calculated from LUMO and optical band gap (E_g) of the synthesized compounds, HOMO = LUMO − E_g (eV). [f]Calculated from the empirical formula, LUMO = $-E_{red}$ − 4.80 (eV).[13]

PL spectra of the synthesized polymers were measured in THF (1×10^{-5} M) and the thin-film states upon the excitation at each absorption maximum (Figure 4c and Table 5). As the typical AIE behavior, the thin film showed large increases in the emission efficiencies, while they showed weak luminescence in the solution states ($\Phi < 0.01$). In addition, the peak positions in the emission band (λ_{PL}) showed good correlation with the order of their E_g values. Moreover, the emission colors were varied from green to red by changing the substituents at the boron diiminate unit. The polymer formed an amorphous state

dx.doi.org/10.1021/ja510985v | J. Am. Chem. Soc. 2014, 136, 18131−18139

Table 5. Optical Properties of Boron Fluorene Polymers

compounds	$\lambda_{abs,THF}$ [nm]	$\lambda_{abs,film}$ [nm]	$\varepsilon \times 10^4$ [M^{-1} cm^{-1}][a]	$\lambda_{PL,film}$ [nm][b,c]	$\Phi_{PL,film}$[b,c,d]
P-H(Me)	374	370	6.34	509	0.11
P-H(Ph)	399	396	5.99	542	0.07
P-OMe	396	393	6.07	542	0.04
P-NO_2	407	405	5.80	575	0.05
P-NMe_2	392	391	6.06	628	0.02

[a]Molar absorption coefficients of the absorption maxima at longer wavelength region. [b]Excited at $\lambda_{abs,film}$. [c]Measured in thin-film states. [d]Determined using integrated sphere method.

(Figure S4). Furthermore, all films of the polymers exhibited higher emission efficiencies (Φ_{PL} = 0.02−0.11) relative to the corresponding amorphous samples of boron diiminates. These results show that the conjugation with fluorene contributes to the improvement of the molar absorption coefficient and the emission intensity.

Finally, the dynamic modulation of the optical properties was performed by acid and base sensing experiments using trifluoroacetic acid (TFA) and triethylamine (NEt_3), respectively. The film of **P-NMe_2** showed red-shifted absorption and PL spectra in comparison with the others because of the strong donor−acceptor interaction (Figure 5). On the other hand, when the **P-NMe_2** film was placed in a small container saturated with TFA vapors, the fumed film showed blue-shifted absorption and emission spectra than those of the parent samples. In the absorption spectra, while the absorption around 500 nm decreased, the absorption around 400 nm increased after the exposure with TFA. These data indicate that the optical properties of boron diiminates-containing polymers can be dynamically regulated in the film states. The strong donor−acceptor interaction between the amino group and the boron chelating ring could be suppressed by the protonation of the amino group (Figure 5c). As a result, the color was changed from orange to yellow. In the PL spectra, the emission of **P-NMe_2** film also shifted to short-wavelength region after the exposure with TFA to induce the protonation; emission color was changed from red to yellow. Furthermore, the optical properties of the TFA-exposed film were converted back into the parent state again by exposing to NEt_3 vapor. These data clearly show that the optical properties can be tuned reversibly. The boron diiminate-containing polymers could find application as various kinds of film-type optical sensors such as pH-, redox- or temperature-sensors.

CONCLUSION

We present here the unique properties of boron diiminates and demonstrate various functionalization such as the emission color tuning and the effect by the conjugation of boron diiminates with fluorene. The synthesized boron diiminates exhibited AIE and CIEE properties. The emission colors were efficiently modulated by introduction of substituents. Especially, the introduction of strong electron-donating substituents such as dimethylamino group induced large red-shifted emission. It was revealed that the incorporation into the conjugation system significantly influenced the electronic structures of boron diiminates. In this study, the beneficial alteration of optical properties such as the increases of the absorption and emission properties was obtained by employing the polymerization. Finally, the dynamic reversible regulation of the optical properties of the polymer thin film was also accomplished by modulating the electron-donating and -withdrawing capability in the substituents using acid−base

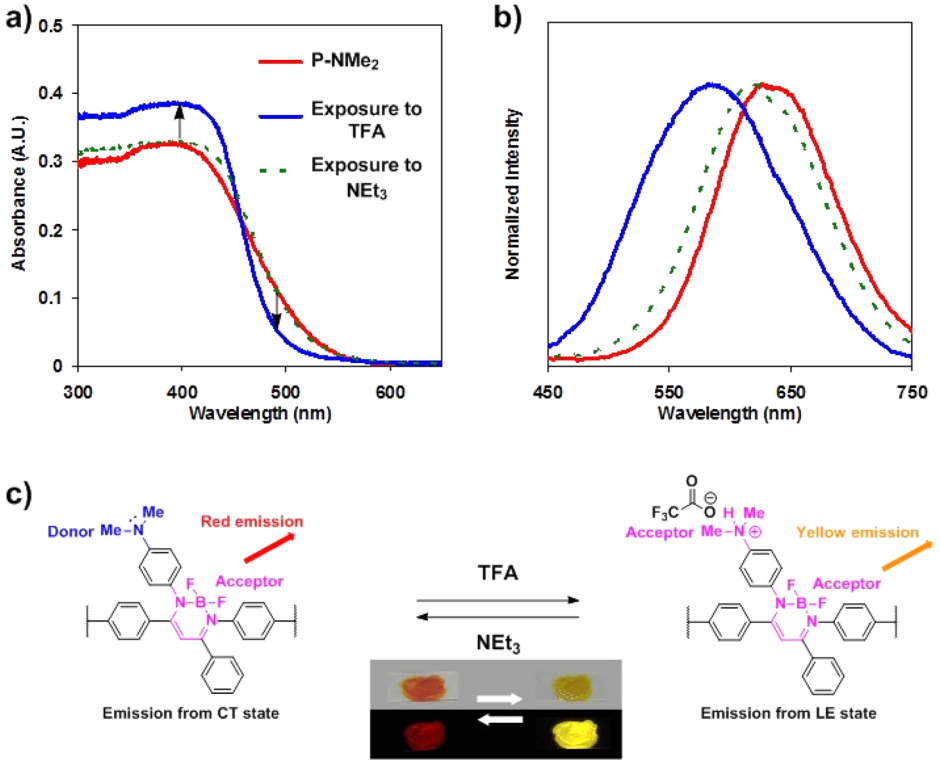

Figure 5. (a) UV−vis absorption and (b) PL spectra of **P-NMe_2** before and after exposure to TFA and NEt_3 vapor in the thin-film state upon excitation at 391 nm. (c) Expected mechanism of the pH-responsive behavior and a photograph of pH sensing.

dx.doi.org/10.1021/ja510985v | J. Am. Chem. Soc. 2014, 136, 18131−18139

interactions. These findings specifically propose that boron diiminates are brilliant organic materials with high functionality involving AIE, CIE, and phosphorescence emissive properties. Such characteristics of boron diiminates might be useful/utilized for developing advanced organic opto and/or electric devices or smart materials such as conjugated polymers, liquid crystal materials, covalent organic framework, and metal organic frameworks, and so on.

■ ASSOCIATED CONTENT

Supporting Information

General, materials, computational details, NMR spectra, CV pots, crystallographic data, UV−vis absorption, and PL data. This material is available free of charge via the Internet at http://pubs.acs.org.

■ AUTHOR INFORMATION

Corresponding Authors

chujo@chujo.synchem.kyoto-u.ac.jp
kazuoppa123@yahoo.co.jp

Notes

The authors declare no competing financial interest.

■ ACKNOWLEDGMENTS

This work was partially supported by the SEI Group CSR Foundation (for K.T.), "the Adaptable and Seamless Technology Transfer Program" through target-driven R&D, Japan Science and Technology Agency (JST), and a Grant-in-Aid for Scientific Research on Innovative Areas "New Polymeric Materials Based on Element-Blocks (no. 2401)" (24102013) of The Ministry of Education, Culture, Sports, Science, and Technology, Japan.

■ REFERENCES

(1) (a) Frath, D.; Massue, J.; Ulrich, G.; Ziessel, R. *Angew. Chem., Int. Ed.* **2014**, *53*, 2290−2310. (b) Tanaka, K.; Chujo, Y. *Macromol. Rapid Commun.* **2012**, *33*, 1235−1255. (c) Li, D.; Zhang, H.; Wang, Y. *Chem. Soc. Rev.* **2013**, *42*, 8416−8433.

(2) (a) Qin, Y.; Kiburu, I.; Shah, S.; Jäkle, F. *Macromolecules* **2006**, *39*, 9041−9048. (b) Cheng, F.; Bonder, E. M.; Salem, S.; Jäkle, F. *Macromolecules* **2013**, *46*, 2905−2915. (c) Chen, P.; Jäkle, F. *J. Am. Chem. Soc.* **2011**, *133*, 20142−20145. (d) Chen, P.; Lalancette, R. A.; Jäkle, F. *J. Am. Chem. Soc.* **2011**, *133*, 8802−8805. (e) Jäkle, F. *Chem. Rev.* **2010**, *110*, 3985−4022. (f) Reus, C.; Guo, F.; John, A.; Winhold, M.; Lerner, H.-W.; Jäkle, F.; Wagner, M. *Macromolecules* **2014**, *47*, 3727−3735.

(3) (a) Zhao, C.-H.; Wakamiya, A.; Yamaguchi, S. *Macromolecules* **2007**, *40*, 3898−3900. (b) Taniguchi, T.; Yamaguchi, S. *Organometallics* **2010**, *29*, 5732−5735. (c) Zhou, Z.; Wakamiya, A.; Kushida, T.; Yamaguchi, S. *J. Am. Chem. Soc.* **2012**, *134*, 4529−4532. (d) Shuto, A.; Kushida, T.; Fukushima, T.; Kaji, H.; Yamaguchi, S. *Org. Lett.* **2013**, *15*, 6234−6237.

(4) (a) Zhang, G.; Chen, J.; Payne, S. J.; Kooi, S. E.; Demas, J. N.; Fraser, C. L. *J. Am. Chem. Soc.* **2007**, *129*, 8942−8943. (b) Zhang, G.; Evans, R. E.; Campbell, K. A.; Fraser, C. L. *Macromolecules* **2009**, *42*, 8627−8633. (c) Zhang, G.; Lu, J.; Sabat, M.; Fraser, C. L. *J. Am. Chem. Soc.* **2010**, *132*, 2160−2162. (d) Samonina-Kosicka, J.; DeRosa, C. A.; Morris, W. A.; Fan, Z.; Fraser, C. L. *Macromolecules* **2014**, *47*, 3736−3746.

(5) Jenekhe, S. A.; Osaheni, J. A. *Science* **1994**, *265*, 765−768.

(6) (a) Luo, J.; Xie, Z.; Lam, J. W. Y.; Cheng, L.; Tang, B. Z.; Chen, H.; Qiu, C.; Kwok, H. S.; Zhan, X.; Liu, Y.; Zhu, D. *Chem. Commun.* **2001**, 1740−1741. (b) Chen, J.; Law, C. C. W.; Lam, J. W. Y.; Dong, Y. Q.; Lo, S. M. F.; Williams, I. D.; Zhu, D.; Tang, B. Z. *Chem. Mater.* **2003**, *15*, 1535−1546. (c) Chen, J.; Xie, Z.; Lam, J. W. Y.; Law, C. C. W.; Tang, B. Z. *Macromolecules* **2003**, *36*, 1108−1117. (d) Wang, J.; Mei, J.; Hu, R.; Sun, J. Z.; Qin, A.; Tang, B. Z. *J. Am. Chem. Soc.* **2012**, *134*, 9956−9966. (e) Dong, Y.; Lam, J. W. Y.; Qin, A.; Sun, J.; Liu, J.; Li, Z.; Sun, J.; Sung, H. H. Y.; Williams, I. D.; Kwok, H. S.; Tang, B. Z. *Chem. Commun.* **2007**, 3255−3257. (f) Dong, Y.; Lam, J. W. Y.; Qin, A.; Li, Z.; Sun, J.; Sung, H. H.-Y.; Williams, I. D.; Tang, B. Z. *Chem. Commun.* **2007**, 40−42.

(7) (a) Yoshii, R.; Nagai, A.; Tanaka, K.; Chujo, Y. *Chem.—Eur. J.* **2013**, *19*, 4506−4512. (b) Koch, M.; Perumal, K.; Blacque, O.; Garg, J. A.; Saiganesh, R.; Kabilan, S.; Balasubramanian, K. K.; Venkatesan, K. *Angew. Chem., Int. Ed.* **2014**, *53*, 6378−6382. (c) Perumal, K.; Garg, J. A.; Blacque, O.; Saiganesh, R.; Kabilan, S.; Balasubramanian, K. K.; Venkatesan, K. *Chem.—Asian J.* **2012**, *7*, 2670−2677. (d) Zhang, X.; Xie, T.; Cui, M.; Yang, L.; Sun, X.; Jiang, J.; Zhang, G. *ACS Appl. Mater. Interfaces* **2014**, *6*, 2279−2284.

(8) Yoshii, R.; Tanaka, K.; Chujo, Y. *Macromolecules* **2014**, *47*, 2268−2278.

(9) Yoshii, R.; Nagai, A.; Tanaka, K.; Chujo, Y. *Macromol. Rapid Commun.* **2014**, *35*, 1315−1319.

(10) Yoshii, R.; Hirose, A.; Tanaka, K.; Chujo, Y. *Chem.—Eur. J.* **2014**, *20*, 8320−8324.

(11) Macedo, F. P.; Gwengo, C.; Lindeman, S. V.; Smith, M. D.; Gardinier, J. R. *Eur. J. Inorg. Chem.* **2008**, 3200−3211.

(12) (a) Fukuda, M.; Sawada, K.; Yoshino, K. *J. Polym. Sci., Part A: Polym. Chem.* **1993**, *31*, 2465−2471. (b) Scherf, U.; List, E. J. W. *Adv. Mater.* **2002**, *14*, 477−487. (c) Yang, R.; Tian, R.; Yan, J.; Zhang, Y.; Yang, J.; Hou, Q.; Yang, W.; Zhang, C.; Cao, Y. *Macromolecules* **2005**, *38*, 244−253. (d) Lim, E.; Jung, B.-J.; Shim, H.-K. *Macromolecules* **2003**, *36*, 4288−4293. (e) Yeo, H.; Tanaka, K.; Chujo, Y. *Macromolecules* **2013**, *46*, 2599−2605. (f) Yoshii, R.; Nagai, A.; Tanaka, K.; Chujo, Y. *J. Polym. Sci., Part A: Polym. Chem.* **2013**, *51*, 1726−1733.

(13) (a) Chen, C.-P.; Chan, S.-H.; Chao, T.-C.; Ting, C.; Ko, B.-T. *J. Am. Chem. Soc.* **2008**, *130*, 12828−12833. (b) Morisaki, Y.; Ueno, S.; Chujo, Y. *J. Polym. Sci., Part A: Polym. Chem.* **2013**, *51*, 334−339.

(14) Frisch, M. J.; Trucks, G. W.; Schlegel, H. B.; Scuseria, G. E.; Robb, M. A.; Cheeseman, J. R.; Montgomery, J. A., Jr.; Vreven, T.; Kudon, K. N.; Burant, J. C.; Millam, J. M.; Iyenger, S. S.; Tomasi, J.; Barone, V.; Mennucci, B.; Cossi, M.; Scalmani, G.; Rega, N.; Petersson, G. A.; Nakatsuji, H.; Hada, M.; Ehara, M.; Toyoto, K.; Fikuda, R.; Hasegawa, J.; Ishida, M.; Nakajima, T.; Honda, Y.; Kitao, O.; Nakai, H.; Klene, M.; Li, X.; Knox, J. E.; Hratchian, H. P.; Cross, J. B.; Adamo, C.; Jaramillo, J.; Gomperts, R.; Stratmann, R. E.; Yazyev, O.; Austin, A. J.; Cammi, R.; Pomelli, C.; Ochterski, J. W.; Ayala, P. Y.; Morokuma, K.; Voth, G. A.; Salvador, P.; Dannenberg, J. J.; Zakrzewski, V. G.; Dapprich, S.; Daniels, A. D.; Strain, M. C.; Farkas, O.; Malick, D. K.; Rabuck, A. D.; Raghavachari, K.; Foresman, J. B.; Ortiz, J. V.; Cui, Q.; Baboul, A. G.; Clifford, S.; Cioslowsky, J.; Stefanov, B. B.; Liu, G.; Liashenko, A.; Piskorz, P.; Komaromi, I.; Martin, R. L.; Fox, D. J.; Keith, T.; Al-Laham, M. A.; Peng, C. Y.; Nanayakkara, A.; Challacombe, M.; Gill, P. M. W.;Johnson, B.; Chen, W.; Wong, M. W.; Gonzalez, C.; Pople, J. A. *Gaussian 03*, revision D.01; Gaussian, Inc.: Wallingford, CT, 2004.

(15) (a) El-Sayed, M. A. *J. Chem. Phys.* **1964**, *41*, 2462−2467. (b) Dreger, Z. A.; Lang, J. M.; Drickamer, H. G. *J. Phys. Chem.* **1996**, *100*, 4637−4645.